Electronic Supplementary Material (ESI) for Journal of Materials Chemistry C.


# Supplementary Information

# Polymer Assisted Transferring of Patterned Electrodes for Weak Anisotropic Charge Transport Study in Monolayer Molecular Crystals

Xiaotong Zhao‡[ab], Jie Liu‡[bc], Jie Liu[b], Haiyang Li[b], Jiajun Zhang[d], Chunlei Li[b], Yicai Dong[b], Xiaosong Shi[b], Yanan Sun[b], Ji Liu[d], Ming Lei*[a] and Lang Jiang*[b]

[a]State Key Laboratory of Information Photonics and Optical Communications & School of Science, Beijing University of Posts and Telecommunications, Beijing 100876, China. E-mail: mlei@bupt.edu.cn

[b]Beijing National Laboratory for Molecular Sciences, Key Laboratory of Organic Solids, Institute of Chemistry, Chinese Academy of Sciences, Beijing 100190, China. E-mail: ljiang@iccas.ac.cn

[c]Life and Health Research Institute School of Chemistry and Chemical Engineering, Tianjin University of Technology, Tianjin 300384, China.

[d]Department of Mechanical and Energy Engineering, Southern University of Science and Technology, Shenzhen 518055, China.

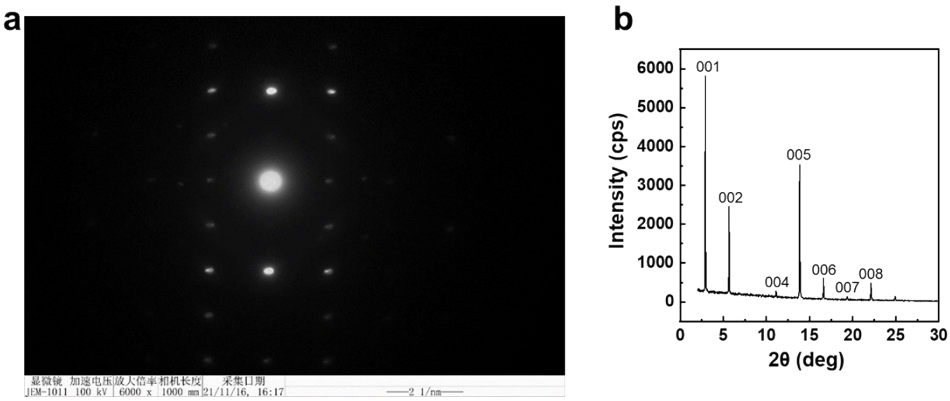


**Figure S1** (a) SAED patterns of C6-DPA MMC. (b) X-ray diffraction pattern of C6-DPA multilayer crystals. The d spacing is 3.0 nm.

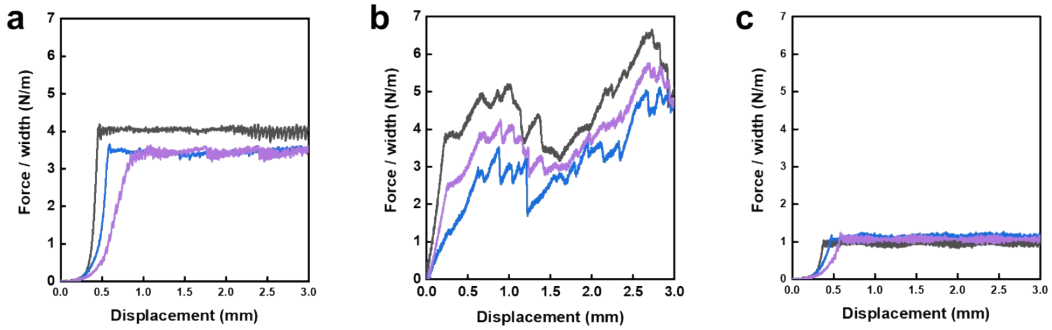


**Fig. S2** Representative curves of the peeling force per width of interface adhesion versus displacement for the 90° peeling tests for three different samples. a) OTS-CYTOP interface; b) $SiO_2$-Au interface; c) OTS-Au interface.

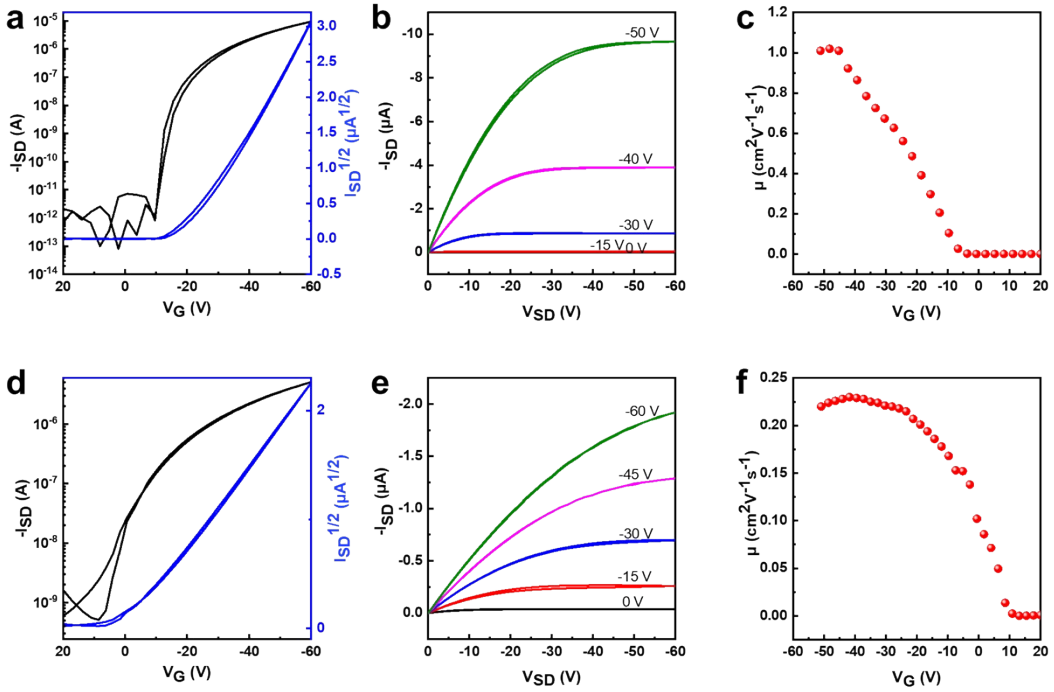


**Fig. S3** Typical electrical characteristics of C6-DPA and HTEB MMC OFETs constructed by the traditional mechanical transfer of gold strips on MMC. (a) Transfer and (b) output characteristics in the saturation regime of the fabricated 1L C6DPA OFET with W/L=1.3. (c) Gate voltage dependence of carrier mobility of 1L C6DPA OFET. (d) Transfer and (e) output characteristics in the saturation regime of the fabricated 1L HTEB OFET with W/L=1. (c) Gate voltage dependence of carrier mobility of 1L HTEB OFET.

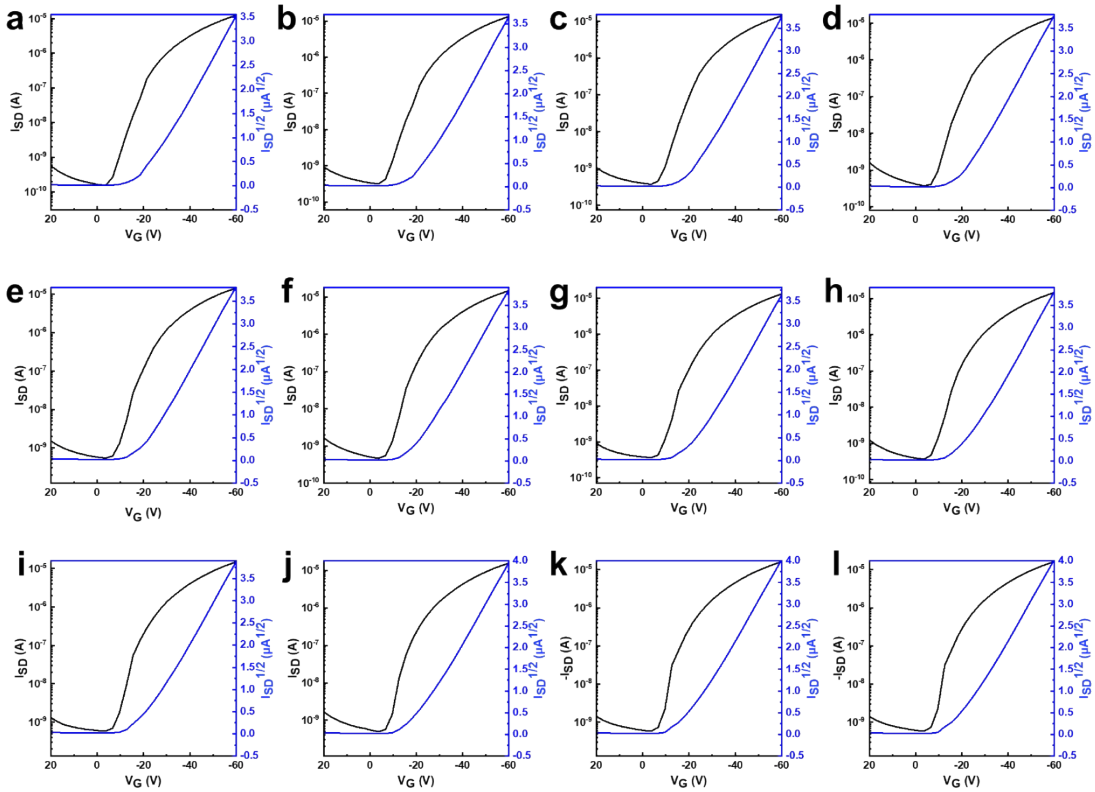


**Fig. S4** Experimental results of the angular-dependent transfer characteristics of the C6DPA MMC OFET in the range of 0-360°, corresponding to a-l, respectively.

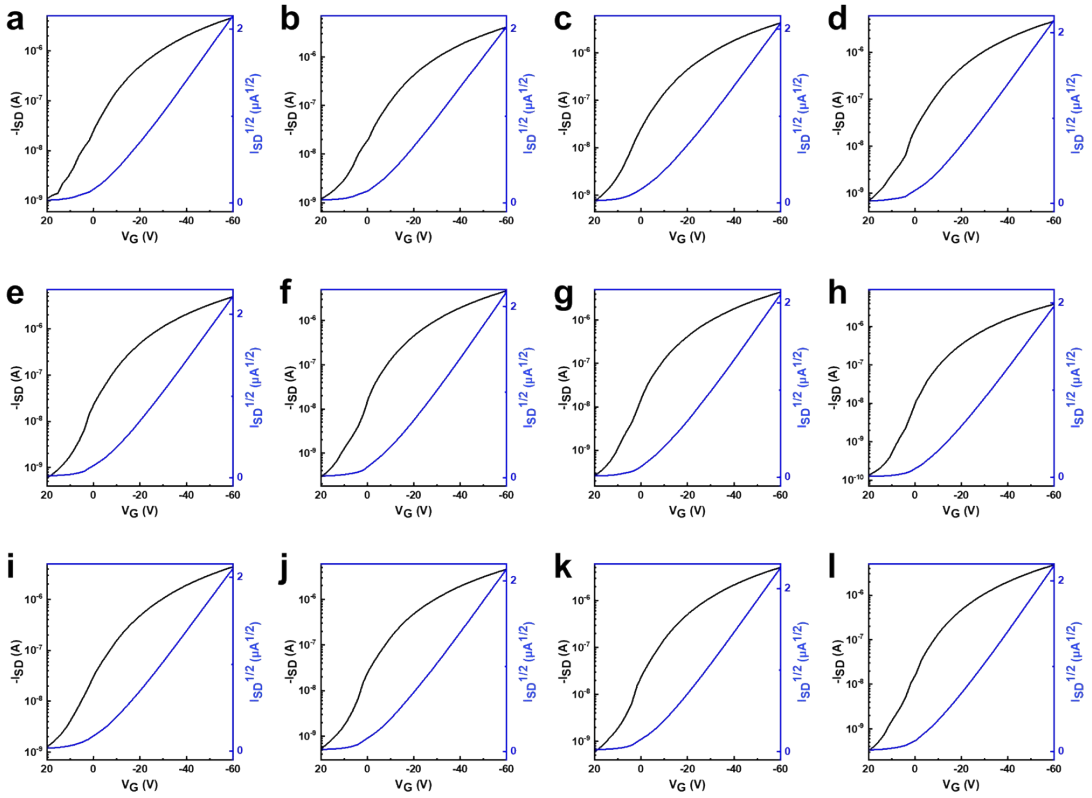


**Fig. S5** Experimental results of the angular-dependent transfer characteristics of the HTEB MMC OFET in the range of 0-360°, corresponding to a-l, respectively.

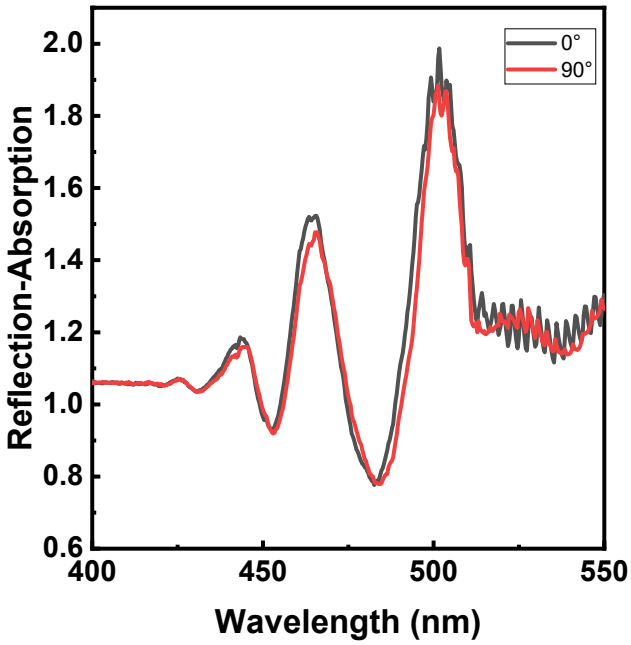


**Fig. S6** Polarized reflection-absorption spectra of C6-DPA MMC.

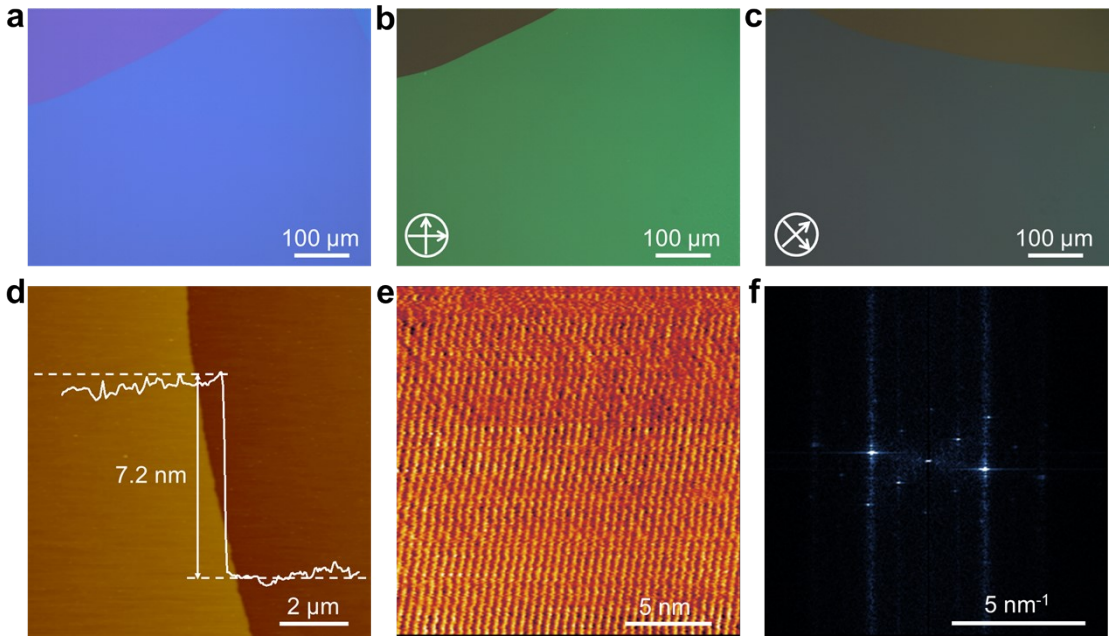


**Fig. S7** (a) OM image of millimeter scale triple-layer C6-DPA molecular crystal. (b, c) The POM image of triple-layer C6-DPA molecular crystal. (d) AFM image and cross-sectional profile of the 3L single crystal. (e) HRAFM image of triple-layer C6-DPA molecular crystal and (f) the corresponding FFT graph.

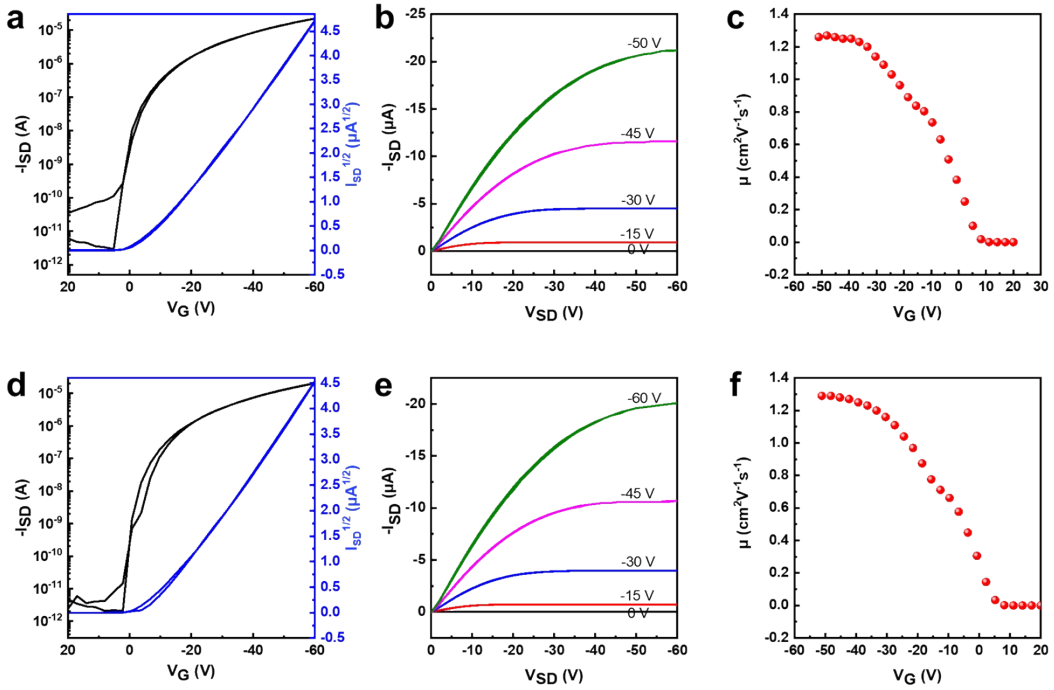


**Fig. S8** Typical electrical characteristics of triple-layer C6-DPA OFETs. (a-c) polymer assisted transferring of patterned electrodes on triple-layer C6-DPA; (d-f) traditional mechanical transfer of gold strips on triple-layer C6-DPA.

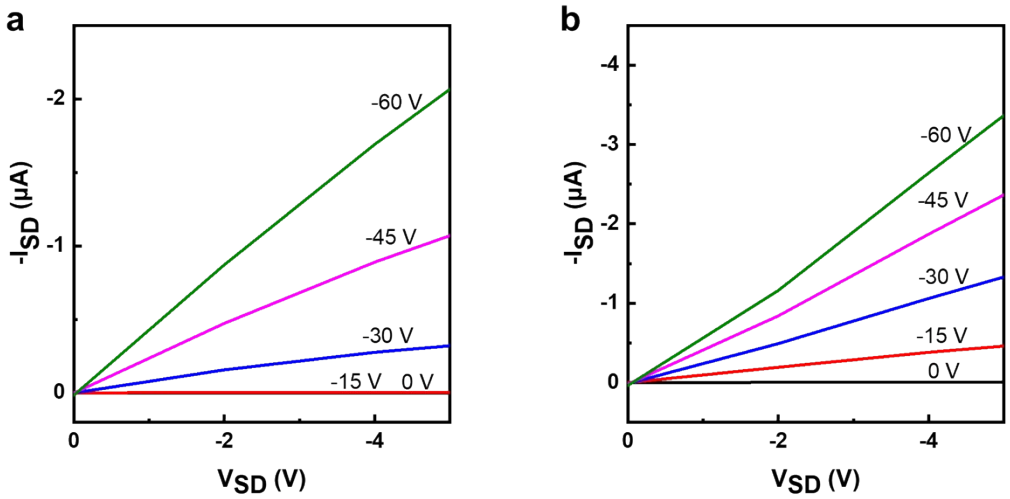


**Fig. S9** (a, b) Output characteristics of the fabricated 1L C6-DPA OFET and 3L C6-DPA OFET under a low $V_{SD}$ of -5V, respectively.

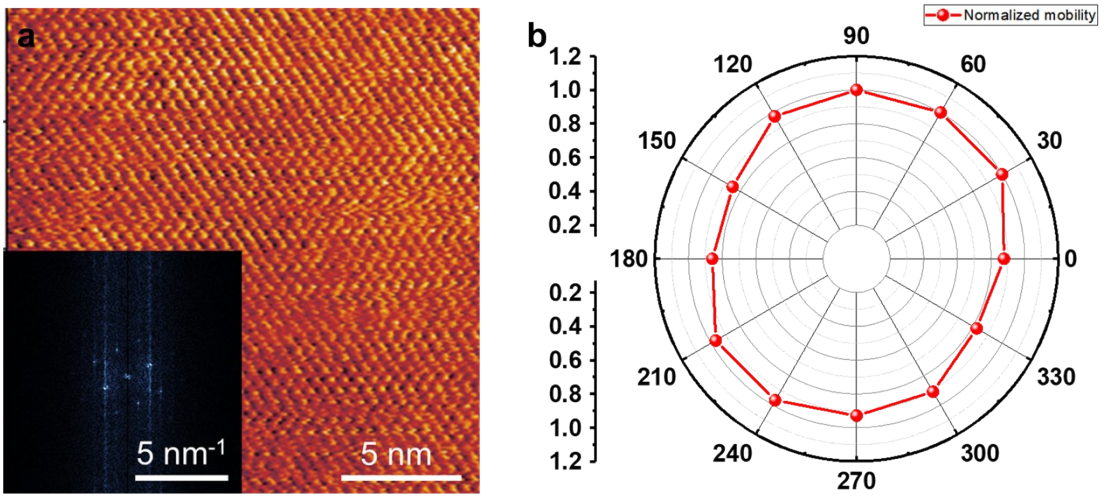


**Fig. S10** (a) HRAFM image in triple-layer C6-DPA molecular crystal and the corresponding FFT graph. (b) Radar graph of normalized mobilities on different directions of triple-layer C6-DPA molecular crystal and anisotropic ratio of 1.21 is obtained.

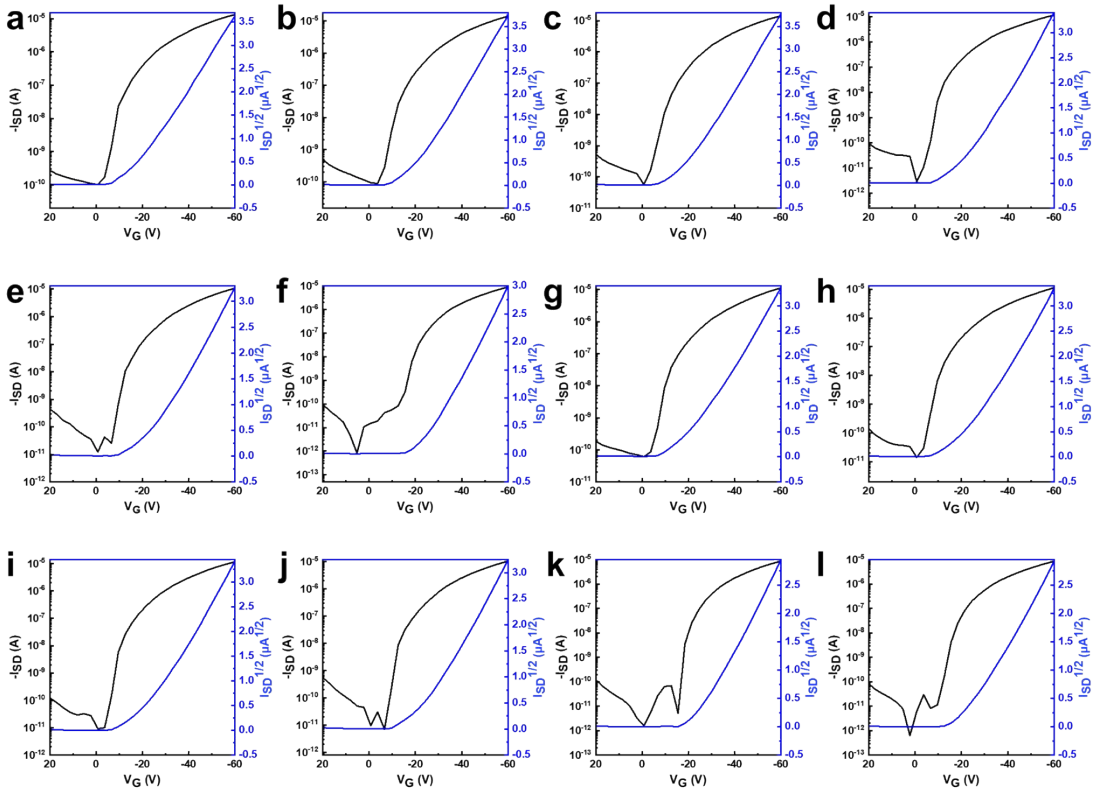


**Fig. S11** Experimental results of the angular-dependent transfer characteristics of the triple-layer C6-DPA OFET in the range of 0-360°, corresponding to a-l, respectively.